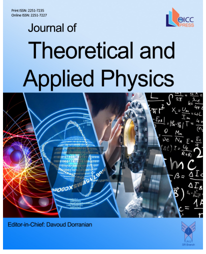

Volume 19, Issue 3, 192530 (1-10)

Journal of Theoretical and Applied Physics (JTAP)

https://doi.org/10.57647/j.jtap.2025.1903.30

Optimizing gliding arc plasma treatment factors for enhanced brake pad performance: Central composite design approach

Ali Partovinia[1,*], Fatemeh Mollaei[2], Saeed Javadi Anaghizi[3], Hamid Ghomi[4]

[1] *Department of Biorefinery, Faculty of New Technologies Engineering, Zirab Campus, Shahid Beheshti University, Tehran, Iran.*
[2] *Research and Development Expert, Remapuya Company, Tehran, Iran.*
[3] *Central Laboratory of Shahid Beheshti University, Tehran, Iran.*
[4] *Laser and Plasma Research Institute, Shahid Beheshti University, Tehran, Iran.*

*__Corresponding author:__ a_partovi@sbu.ac.ir

Original Research

Received:
12 June 2025
Revised:
21 June 2025
Accepted:
25 June 2025
Published online:
30 June 2025

Abstract:

Brake pad quality is crucial for vehicle safety, as it requires stable friction coefficients, appropriate wear rates, and consistent performance across varying temperatures, pressures, and speeds. This study examines the impact of gliding arc plasma treatment on tribological properties and wear behavior of the brake pads. In this research, three key parameters of treatment time (60 – 180 s), treatment distance (2 – 4 cm), and input power (1.5 – 4.5 kW) were optimized using response surface methodology (RSM) with a central composite design (CCD). Analysis of variance (ANOVA) for the quadratic model revealed that gliding arc plasma treatment duration significantly influenced normal and hot friction levels. At the same time, interactions between time-distance and time-input power affected normal and hot friction, respectively. The optimal conditions were achieved at 180 seconds of treatment time, 3.77 cm distance, and 4.20 kW power. Linear model analysis of wear indicated that input power was the only statistically significant main factor. These findings demonstrate that gliding arc plasma treatment parameters not only individually influence tribological behavior but also interact synergistically, offering valuable insights for industrial brake pad manufacturing.

Keywords: Gliding arc plasma; Friction coefficient; Wear resistance; Design of experiment

1. Introduction

In the automotive industry, brake pads play a critical role in braking systems to control the speed of vehicles, automobiles, and machines [1]. The braking system converts the kinetic energy of vehicles into thermal energy and finally releases it into the atmosphere. The brake system consists of a disc and a brake pad connected to the hub through a caliper [2]. The brake pad is made of a steel back plate and friction materials that can be various for different types of cars [3]. The brake pad is generally classified into three types: metallic, non-metallic, and non-asbestos organic (NAO). Friction material (FM) is the heart of the braking system and is divided into five main classes of materials: binder, reinforcing fibers, functional fillers, friction modifiers, and abrasive [4].

FMs are important for the moderate and stable value of the friction coefficient (μ), which will be least sensitive to the various operating conditions, resistance (as high as possible) to fade, wear, and squeal. Chan and Stachowiak (2004) examined the phase-out of asbestos and provided a comprehensive analysis of modern dry and wet automotive brake friction materials, detailing the advantages and limitations of their typical ingredients and formulations. Kchaou and colleagues (2019) demonstrated that accurately characterizing brake friction materials requires a combination of full-scale and reduced-scale tribological tests, along with distinct definitions for minimum, maximum, and average coefficients of friction to capture performance across varying thermal and mechanical conditions. For safety braking systems, normal and hot friction stability are very important. Industries are seriously concerned about wear. Also, particles caused by wear are one of the most important sources related to non-exhaust and the emission of suspended particles. In various fields, many researchers seek to reduce wear by adding or removing some materials. For instance, Takashima and Ohtake (2011) demonstrated that using a Cr/Si-C:H dual interlayer improves the adhesion, wear resistance, and corrosion protection of Diamond-like carbon (DLC) coatings on stainless steel. DLC coatings are currently being used in a wide variety of industrial fields because of their outstanding properties, such as high hardness and low friction, among others. Beake et al. (1998) show that argon plasma treatment increases surface polarity and friction of PET by modifying its chemistry and energy, as revealed through chemical force microscopy [5–9]. Also, for the development of brake pads, in addition to the lower rate of wear, it is important to pay attention to the stable friction coefficient at high speed, pressure, and temperature [10].

Plasma has been utilized in previous studies to decrease wear and stabilize the friction coefficient. Plasma is an ionized gas with balanced positive and negative charges, capable of existing across a wide range of temperatures and pressures, and is often used to enhance surface properties. Mahale and Bijwe (2020) have used plasma to treat the surface of brake pads and reduce wear [11, 12]. In another study, Kalel and coworkers used low-pressure argon plasma to reduce brake pad wear. Their goal was to enhance surface resistance and minimize the wear rate during operation [13]. In addition, a group of researchers studied how plasma treatment influences the adhesion, friction, and wear behavior of polymer coatings by modifying surface energy and enhancing interfacial bonding with various substrates. Samad et al. (2010) showed that air plasma pre-treatment significantly improves the adhesion strength and tribological performance of Ultra High Molecular Weight Polyethylene (UHMWPE) films on silicon substrates, resulting in much greater wear resistance compared to conventional chemical methods. Additionally, Liston et al. (1989) provided a comprehensive review of low-pressure glow discharge plasma treatments, describing equipment types, operating parameters, and fundamental mechanisms, and emphasized their effectiveness in promoting material bonding through improved surface activation and cleaning [14–16].

In the process of friction and wear, a geometric adaptation occurs between the brake pad and the disc, which causes full contact between the brake pad and the disc, which is called bedding. In other words, bedding is a term used to describe the performance of new brake pads. Besides, the scorching process involves burning off a thin layer of the friction material—ranging from a few hundred micrometers to about one millimeter—which enhances contact with the disc, improves initial braking performance, and reduces bedding time. This means that the pad and disc need less time to get matched to each other. The scorching process requires a high temperature and a long time, so plasma can be used instead of this process, which improves the properties of the surface and bedding in new brake pads in a shorter period and under more convenient conditions [17, 18].

This survey investigates the effect of different factors of gliding arc plasma, including time, distance, and input power, on important braking parameters such as wear rate, normal friction, and hot friction coefficients. In addition, the optimal plasma parameters have also been determined to ensure the best performance in terms of wear rate and friction coefficients. Furthermore, the benefits of substituting plasma instead of the scorch process and the effect of plasma on bedding have been investigated.

2. Materials and methods

2.1 Materials and instruments

The primary materials used in the samples were sourced from the Remapouya factory (Tehran, Iran). The composition of the brake pads consists of a mixture of binder, reinforcing fibers, functional fillers, friction modifiers, and abrasives [19–21]. All samples were prepared using an identical formulation, with gliding arc plasma surface treatment being the sole variable in the manufacturing process. The pre-mixed materials underwent hot molding at 170 °C under a pressure of 2.81 kN/cm^2 for 5 minutes. Subsequently, a post-curing process was carried out at 140 – 180 °C for 8 hours to ensure optimal thermosetting and mechanical properties. These processing conditions were selected based on typical industrial applications.

2.2 Gliding arc plasma treatment procedures

Each sample was uniformly cut to dimensions of 25 $\times$ 25 mm and then curved, with a thickness of approximately 6 mm at the center. Before gliding arc plasma treatment, the samples were conditioned on a Chase testing machine for

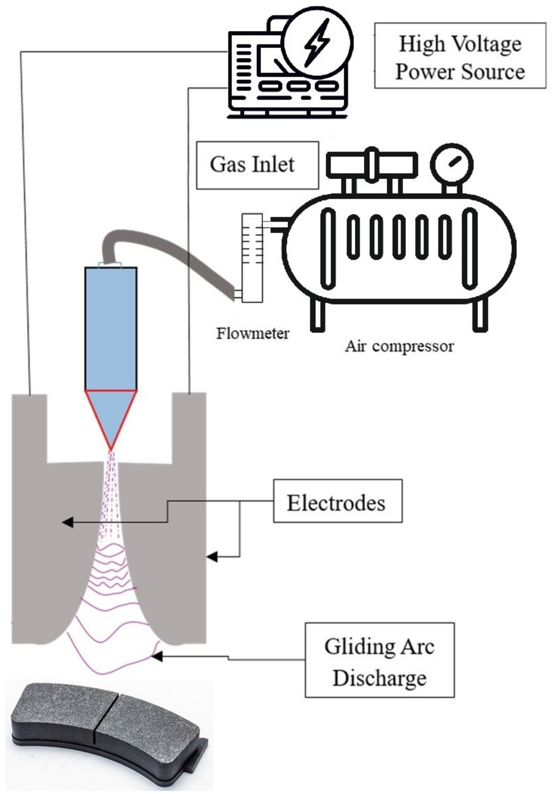

Figure 1. Scheme of the gliding arc plasma treatment.

1200 seconds to ensure surface stabilization. Following conditioning, the samples were thoroughly cleaned to remove any contaminants. Gliding arc plasma treatment was then performed using a Plasmatek-15B system, (figure 1), with the operational parameters detailed in Table 1.

2.3 Experimental methodology

Three critical factors of gliding arc plasma treatment were systematically investigated using a Design of Experiments (DOE) approach (Design-Expert software, version 7.0.0). The treatment time (A: $60-180$ seconds), distance (B: $2-4$ cm), and input power (C: $1.5-4.2$ kW) were selected based on preliminary screening experiments conducted to identify effective and practical ranges for the process parameters. The study used a hybrid design combining full factorial and central composite design (CCD) methods. It included 8 factorial points, 6 axial points, and 3 center point replicates, totaling 17 randomized runs. This setup ensured rotatability and allowed thorough evaluation of main effects and interactions in a three-factor system. This optimized design matrix, presented in Table 2, provides balanced coverage of the design space while maintaining statistical efficiency for subsequent response surface analysis [22].
The experimental data were analyzed using response surface methodology (RSM), which fits a quadratic polynomial equation to model the relationship between input factors (A,

Table 1. Technical specifications of the gliding arc plasma treatment system.

Item	Specification
Dimensions	45 (W) × 65 (D) × 55 (H) cm
Weight	Approx. 70 kg
Input specification	AC 220 V, 50 Hz, 1 Phase
Input power	3000 W
Plasma distance	Adjustable
Treatment area size	Adjustable
Plasma probe dimension	8.5 cm × 7 cm × 3.5 cm
Plasma length	110 mm
Plasma width	40 mm

Table 2. Experimental design matrix for gliding arc plasma treatment parameters.

Run Order	Time (A) (s)	Distance (B) (cm)	Power (C) (kW)
1	60	4	4.20
2	60	3	2.85
3	60	4	1.50
4	60	2	1.50
5	60	2	4.20
6	120	4	2.85
7	120	2	2.85
8	120	3	2.85
9	120	3	1.50
10	120	3	4.20
11	120	3	2.85
12	120	3	2.85
13	180	3	2.85
14	180	4	1.50
15	180	4	4.20
16	180	2	4.20
17	180	2	1.50

B, C) and response variables (friction, wear). The general form of the second-order model is expressed as:

$$Y = \beta_0 + \sum(\beta_i X_i) + \sum(\beta_{ii} X_i^2) + \sum(\beta_{ij} X_i X_j) + \varepsilon \quad (1)$$

where Y represents the predicted response (e.g., friction coefficient or wear rate), β_0 is the constant term (intercept), β_i are the linear coefficients for factors (A, B, C), β_{ii} are the quadratic coefficients (capturing curvature effects), β_{ij} are the interaction coefficients (e.g., A $\times$ B, A $\times$ C, B $\times$ C), X_i are the coded variables (-1, 0, $+1$) for factors A, B, C, and ε represents the random error term [23, 24].

Friction performance and wear characteristics were evaluated using a Chase testing machine by the ISIRI-586 standard. This standard specifies the procedures for testing the friction and wear characteristics of brake linings using a Chase machine, providing a consistent method for evaluating material performance under controlled conditions. It measures friction, fade, recovery, and wear, and assigns friction codes (like FF or GG) for classification. This standard supports quality control and safety in brake system development. The experimental protocol consists of seven distinct test phases designed to assess friction behavior along with wear resistance. Test specimens with dimensions of 25×25 mm (6 mm nominal thickness at center point) were prepared with precision-ground flat surfaces to ensure consistent contact conditions. This standardized methodology enables systematic investigation of gliding arc plasma treatment effects on tribological performance while ensuring experimental reproducibility and data reliability.

3. Results and discussion

A systematic optimization study was conducted to model the influence of gliding arc plasma treatment parameters on critical brake pad characteristics. As detailed in Table 3, three key process variables were investigated to comprehensively evaluate both individual and interactive effects of gliding arc plasma surface modification on tribological performance metrics.

The experimental methodology facilitates a comprehensive analysis of parameter-response relationships, enabling systematic optimization of brake pad performance characteristics. Through iterative testing and response surface analysis, we established statistically significant correlations between gliding arc plasma treatment parameters and critical performance metrics. As shown in Table 4, the measured responses, including normal and hot friction coefficients and wear rate, are demonstrated.

Table 3. Experimental design factors with coded levels and actual ranges.

Factor	Level (-1)	Level (0)	Level ($+1$)	Unit
A: Treatment time (s)	60	120	180	s
B: Distance (cm)	2	3	4	cm
C: Input power (kW)	1.50	2.85	4.20	kW

Table 4. Experimental design matrix and measured responses for gliding arc plasma-treated brake pads.

Run No.	Factors			Responses		
	Time (s)	Distance (cm)	Input power (kW)	Normal friction	Hot friction	Wear (%)
1	60	4	4.20	0.439	0.384	1.97
2	120	4	2.85	0.397	0.394	3.35
3	120	2	2.85	0.417	0.405	3.72
4	180	3	2.85	0.53	0.463	5.59
5	60	3	2.85	0.424	0.417	3.36
6	180	4	1.50	0.51	0.451	5.56
7	180	4	4.20	0.544	0.463	4.6
8	120	3	2.85	0.537	0.439	4.51
9	120	3	1.50	0.56	0.443	4.74
10	120	3	4.20	0.52	0.432	2.35
11	180	2	4.20	0.472	0.439	4.88
12	60	4	1.50	0.395	0.444	4.36
13	120	3	2.85	0.514	0.424	5.31
14	120	3	2.85	0.448	0.412	2.78
15	60	2	1.50	0.506	0.416	6.68
16	60	2	4.20	0.47	0.419	4.56
17	180	2	1.50	0.519	0.434	5.26

3.1 Friction characteristics: Coefficient analysis

The statistical analysis presented in Table 5 demonstrates that among all investigated factors, gliding arc plasma treatment time (A) has a significant impact and the interaction between time and distance has a possibly significant effect on normal friction coefficient. The remaining factors, exhibiting p-values greater than the 0.1 significance threshold, were identified as non-significant contributors and consequently excluded from the final model to maintain model simplicity and predictive reliability. This approach follows established design of experiments principles for optimizing model accuracy while eliminating redundant variables. While the statistical results highlight the significance of treatment time and its interaction with distance, it should be noted that the present study was focused on tribological behavior, and detailed surface morphology analysis was not conducted. Further investigations are needed to correlate these effects with underlying surface modifications.
Figure 2 demonstrates a statistically significant positive correlation between gliding arc plasma treatment time and normal friction coefficient, with longer exposure times resulting in progressively higher normal friction values. The interaction plot in figure 3 reveals a more complex relationship, where the combined effect of treatment time and distance (AB interaction) significantly influences normal friction behavior. Notably, at the minimal gliding arc plasma distance (2 cm), friction coefficients remained relatively stable regardless of treatment time. Conversely, at the maximum tested distance (4 cm), a pronounced time-dependent enhancement of friction characteristics was observed. Although the outcomes of plasma surface treatments can differ based on material properties and experimental parameters, the study conducted by Cai et al. (2020) demonstrated a reduction in friction coefficients for plasma-enhanced alumina (PEA) coated systems in comparison to untreated surfaces. This improvement is attributed to the inherent material-specific interactions between the plasma and the substrate, where unique surface chemistry and morphology of PEA facilitate more effective surface activation and stabilization. These findings emphasize the critical role that intrinsic material characteristics play in dictating the extent and nature of plasma-induced modifications [25]. The discrepancy suggests that the tribological effects of plasma treatment may be highly dependent on both substrate material and treatment parameters, emphasizing the need for system-specific optimization.
As presented in Table 6, the analysis of variance identifies two parameters with significant effects on hot friction performance, including treatment time (A) and the time–power interaction (AC). These results highlight the dominant role of temporal exposure and its synergistic relationship with gliding arc plasma power input in controlling elevated-temperature friction behavior. The remaining factors, exhibiting p-values above the 0.1 significance threshold, demonstrated negligible influence and were consequently excluded from the refined model.
Figure 4 shows the behavior of hot friction changes over time, showing a clear response, unlike the steady relationship seen with normal friction. Initially, up to approximately 90 seconds, the hot friction coefficient remains stable without any significant changes. However, after this period, it shows a significant increase. Additionally, the significant interaction between time and input power shows that hot friction increased in both low and high-power settings. However, an increase in input power, particularly at 4.2 kW, led to a significant rise in the hot friction coefficient

Table 5. Analysis of variance of normal friction response.

Source	Sum of squares	df	Mean square	F Value	p-value	Significance status
Model	0.0392	9	0.0044	4.44	0.0311	S
A-Time	0.0116	1	0.0116	11.85	0.0108	S
B-Distance	0.0010	1	0.0010	0.999	0.3509	NS
C-Input Power	0.0002	1	0.0002	0.206	0.6634	NS
AB	0.0053	1	0.0053	5.353	0.0539	PS
AC	6E-05	1	6E-05	0.056	0.8194	NS
BC	0.0032	1	0.0032	3.302	0.1120	NS
A^2	3E-08	1	3E-08	3E-05	0.9957	NS
B^2	0.0132	1	0.0132	13.42	0.0080	HS
C^2	0.0106	1	0.0106	10.8	0.0134	S
Residual	0.0069	7	0.0010			
Lack of Fit	0.0026	5	0.0005	0.244	0.9118	NS
Pure Error	0.0043	2	0.0021			
Cor Total	0.0461	16				

S: significant, HS: highly significant, NS: not significant, PS: possibly significant

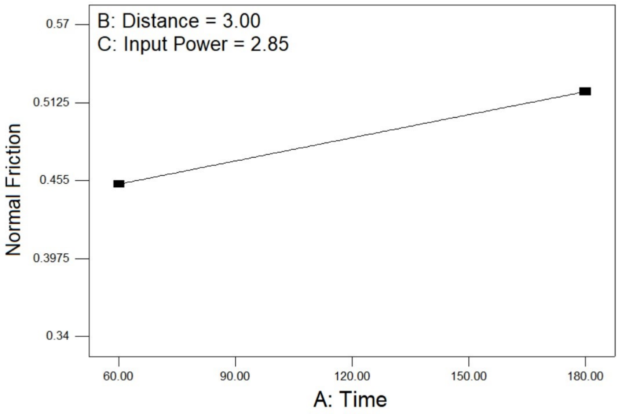

Figure 2. Effect of plasma treatment time (Factor A) on normal friction coefficient (NF).

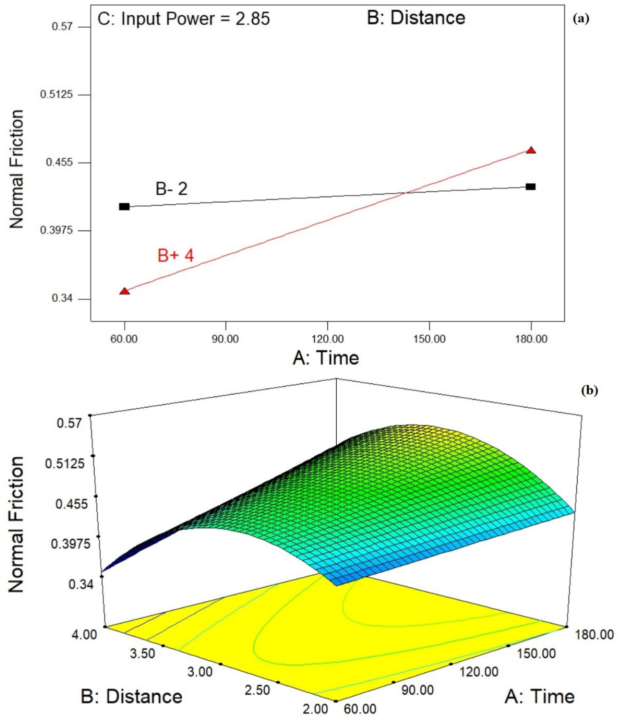

Figure 3. (a) Interaction and (b) 3D surface plot of plasma treatment time (A) and nozzle distance (B) on normal friction coefficient (NF).

(figure 5). This suggests that the behavior is a key feature of how plasma modifies surfaces.

Comparative analysis with existing literature reveals several noteworthy observations. Mahale and Bijwe (2020) reported that enhanced frictional performance in treated stainless steel brake pads, particularly under high deceleration conditions, was attributed due to treatment-induced adhesion enhancement [11]. In contrast, the investigations by Cai and colleagues on plasma-enhanced alumina coatings showed slightly lower but more consistent friction coefficients in treated cast iron systems [26]. These apparent contradictions highlight the material-specific nature of plasma treatment effects and underscore the importance of considering individual parameter effects and their complex interdependencies. While earlier studies have mainly concentrated on changes in wear rate, the present research highlights the significant role of gliding arc plasma treatment in altering both normal and hot friction behavior, offering new insights into surface performance enhancement.

These friction modifications likely originate from gliding arc plasma-induced alterations in surface morphology, interfacial adhesion properties, and microstructural evolution. The potential formation of nanoscale may further contribute to the observed friction behavior. Although the present study focused on performance-based evaluations, further characterization using techniques such as XPS or FTIR is recommended to investigate the chemical changes induced by plasma treatment on the material surface.

Table 6. Analysis of variance of hot friction response.

Source	Sum of squares	df	Mean square	F Value	p-value	Significance status
Model	0.0068	9	0.0008	4.288	0.0340	S
A-Time	0.0029	1	0.0029	16.49	0.0048	HS
B-Distance	5E-05	1	5E-05	0.302	0.5999	NS
C-Input Power	0.0003	1	0.0003	1.484	0.2626	NS
AB	0.0003	1	0.0003	1.643	0.2407	NS
AC	0.0007	1	0.0007	3.905	0.0887	PS
BC	0.0004	1	0.0004	2.236	0.1785	NS
A^2	0.0007	1	0.0007	4.25	0.0782	PS
B^2	0.0015	1	0.0015	8.675	0.0216	S
C^2	0.0005	1	0.0005	3.071	0.1231	NS
Residual	0.0012	7	0.0002			
Lack of Fit	0.0009	5	0.0002	0.941	0.5875	NS
Pure Error	0.0004	2	0.0002			
Cor Total	0.008	16				

S: significant, HS: highly significant, NS: not significant, PS: possibly significant

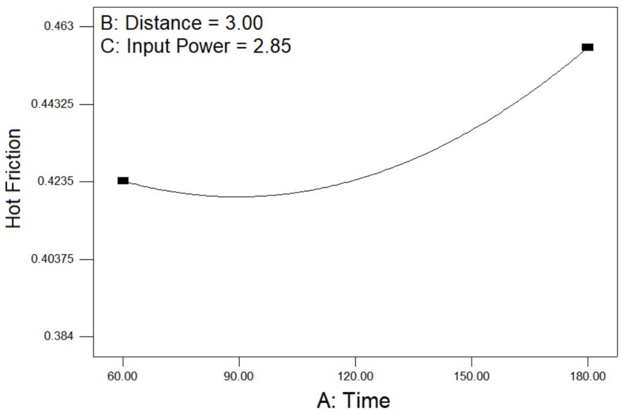

Figure 4. Effect of plasma treatment duration (Factor A) on hot friction coefficient (HF).

3.2 Wear analysis

Statistical analysis of wear behavior (Table 7) reveals that gliding arc plasma input power (C) serves as the sole significant factor of wear performance, exhibiting a statistically robust influence. The non-significant p-values associated with the remaining parameters justify their exclusion from the final predictive model.

Effect of plasma input power (C) on wear rate at fixed treatment time (120 s) and distance (3 cm), demonstrating significant inverse correlation ($p < 0.05$). The plot confirms input power as the dominant wear-determining factor, consistent with the ANOVA results is demonstrated in Table 7. Specifically, the wear rate decreases with increasing gliding arc plasma input power (figure 6). Comparative literature analysis reveals that plasma treatment enhances wear resistance through interfacial modification. In previous studies by Kalel et al. (2022) and Mahale and Bijwe (2020) reported that improved wear performance in treated systems, attributed to strengthened matrix adhesion. Previous studies further support this understanding by demonstrating modified interfacial characteristics in plasma-treated systems [11, 13, 26]. Notably, the DLC-coated rubber with Ar plasma pretreatment demonstrated a consistently low friction coefficient of 0.19 and excellent wear resistance. This

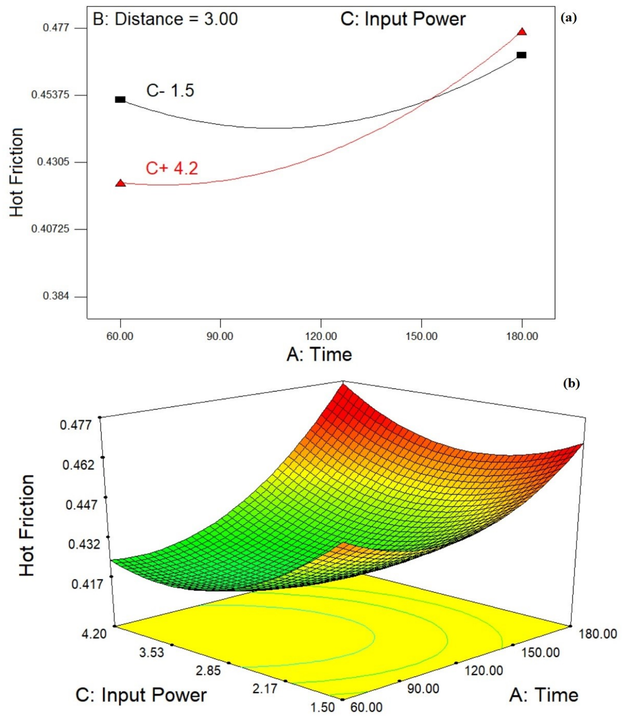

Figure 5. (a) Interaction and (b) 3D surface plot of plasma treatment time (A) and input power (C) on hot friction coefficient (HF).

performance was attributed to strong adhesion, enhanced load-bearing capacity of the rubber surface, and the near-sinusoidal surface profile of the DLC film [27]. Further investigations, including microhardness analysis to assess surface hardening effects, are recommended for future studies based on the observations made during this work.

3.3 Gliding arc plasma treatment over scorch process in brake bedding performance

Gliding arc plasma treatment demonstrates superior performance in the brake bedding process compared to traditional scorch methods, offering faster, more stable, and predictable results. During bedding-the critical break-in period where brake pads and rotors establish optimal contact–gliding arc plasma-treated surfaces achieve more consistent friction

Table 7. Analysis of variance of wear response.

Source	Sum of squares	df	Mean square	F Value	p-value	Significance status
Model	12.017	3	4.0056	3.937	0.0336	S
A-Time	2.4602	1	2.4602	2.418	0.1440	NS
B-Distance	2.7668	1	2.7668	2.719	0.1231	NS
C-Input Power	6.7898	1	6.7898	6.673	0.0227	S
Residual	13.227	13	1.0175			
Lack of Fit	9.8826	11	0.8984	0.537	0.7988	NS
Pure Error	3.3446	2	1.6723			
Cor Total	25.244	16				

S: significant, NS: not significant

coefficients (μ) right from the initial bedding phase, with an average μ of 0.499 and only $+12.6\%$ variation, versus scorch-treated materials that show unstable μ averaging 0.325 with erratic fluctuations (Table 8). This stability allows gliding arc plasma-treated brakes to complete the bedding process more efficiently, as evidenced by their uniform wear pattern (0.13 mm thickness loss distributed evenly) compared to scorch's less predictable wear (0.10 mm loss but with inconsistent contact patch formation).
The key advantage lies in the gliding arc plasma's ability to maintain thermal stability throughout the bedding process. While both processes show initial wear, gliding arc plasma-treated pads recover faster after heat cycles and maintain consistent performance, enabling quicker establishment of the ideal pad-to-rotor interface. Scorch methods, in contrast, suffer from prolonged recovery times and thermal inconsistency, delaying proper bedding. This makes gliding arc plasma particularly valuable for high-performance applications where immediate, reliable braking is crucial after installation. Meanwhile, understanding the complex interactions at the contact interface between brake materials and their counterparts is essential for optimizing braking performance. Eriksson and Jacobson (2000) showed that friction layers formed from wear debris on organic brake pads play a key role in determining their tribological performance under varying braking conditions [28]. Österle and Dmitriev (2011) studied conventional brake friction materials at different scales and demonstrated that understanding both their microstructural and overall behaviors is crucial for improving brake performance and durability [29].
In conclusion, gliding arc plasma treatment enhances the bedding process by acting through three distinct mechanisms, including creating a more uniform surface topography from the start, maintaining stable friction characteristics during initial heat cycles, and achieving proper pad-to-rotor conformity in fewer braking applications. These benefits contribute to shorter break-in periods, more consistent performance, and minimized risk of uneven deposits-key considerations for both OEMs and aftermarket use. Although the initial wear is slightly higher (2.775% vs. 1.974% weight loss), the enhanced long-term durability provided by gliding arc plasma treatment (22315 vs. 21327 rotations) outweighs this drawback, positioning it as the more effective solution overall.

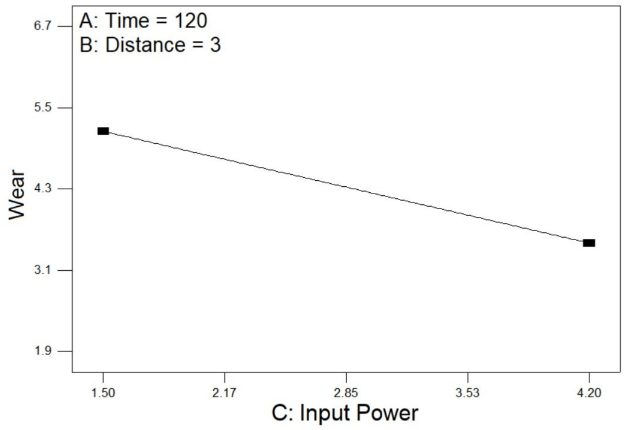

Figure 6. Effect of plasma input power (C) on wear rate.

4. Conclusion

This investigation demonstrates the substantial influence of gliding arc plasma treatment parameters on the tribological performance of brake systems. The systematic analysis reveals that gliding arc plasma exposure time, nozzle-to-sample distance, and energy input collectively affected both frictional behavior and wear resistance through individual and synergistic mechanisms. These findings establish a critical foundation for performance optimization in automotive safety applications. The results

Table 8. Gliding arc plasma vs. scorch performance in brake bedding process.

Performance Metric	Gliding Arc Plasma Treatment	Scorch process	Advantage
Initial Friction (μ)	0.499 (avg)	0.325 (avg)	53.5% higher
Bedding Wear	0.13 mm (uniform)	0.10 mm (inconsistent)	Better contact formation
Weight Loss During Bedding	2.775%	1.974%	Slightly higher but more consistent
Total Endurance (rotations)	22315	21327	4.6% longer lifespan
Bedding Time	Shorter	Prolonged	Quicker to optimal performance
Brake Pads Class	F F	F E	Meets higher standards

showed that the time, distance, and input power, separately and in interaction with each other, affected brake pads' tribological behaviors. The gliding arc plasma treatment time significantly affected both normal and hot frictions of brake pads. Moreover, the input power of gliding arc plasma affected the wear response. The optimum condition was determined in 180 s, with 4.20 kW of input power and at a sample distance of 3.77 cm. Finally, we concluded that this treatment outperforms scorch processing in brake bedding by delivering 53.5% higher initial friction, more stable performance, and superior thermal recovery while maintaining long-term durability, making it the superior choice for modern braking systems.

Acknowledgement
This work was financially supported by Remapuya Industrial Group (Contract no. 1402/11/2/382), which is gratefully acknowledged. We are deeply grateful to Dr. Mohammad Reza Mallaki and Eng. Meysam Mallaki for their exceptional support and unwavering encouragement throughout the development of this work.

Authors Contribution
A. Partovinia: Conceptualization, Supervision, Software, Methodology, Formal Analysis, Review and Editing, Finalizing the paper. F. Mollaei: Investigation, Validation, Formal Analysis, Writing–Original draft. S. Javadi Anaghizi: Conceptualization, Setup design, Methodology, Review and Editing. H. Ghomi: Conceptualization, Supervision, Review and Editing. All the authors read and approved the submission of the manuscript.

Availability of data and materials
The data that support the findings of this study are available from the corresponding author, upon reasonable request.

Conflict of interests
The authors declare that they have no known competing financial interests or personal relationships that could have appeared to influence the work reported in this paper.

References

[1] S. M. Mulani, A. Kumar, H. N. E. A. Shaikh, A. Saurabh, P. K. Singh, and P. C. Verma. "A review on recent development and challenges in automotive brake pad-disc system.". *Materials Today: Proceedings*, **56**:447–454, 2022.
DOI: https://doi.org/10.1016/j.matpr.2022.01.410.

[2] A. Rashid. "Overview of disc brakes and related phenomena-a review. ". *International journal of vehicle noise and vibration*, **10**:257–301, 2014.
DOI: https://doi.org/10.1504/IJVNV.2014.065634.

[3] A. Borawski. "Conventional and unconventional materials used in the production of brake pads–review.". *Science and Engineering of Composite Materials*, **27**:374–396, 2020.
DOI: https://doi.org/10.1515/secm-2020-0041.

[4] R. Ciudin, P. Verma, S. Gialanella, and G. Straffelini. "Wear debris materials from brake systems: environmental and health issues.". *WIT Transactions on Ecology and the Environment*, **191**:1423–1434, 2014.
DOI: https://doi.org/10.2495/SC141202.

[5] M. Kchaou, A. Sellami, J. Fajoui, R. Kus, R. Elleuch, and F. Jacquemin. "Tribological performance characterization of brake friction materials: What test? What coefficient of friction? ". *Proceedings of the Institution of Mechanical Engineers, Part J: Journal of Engineering Tribology*, **233**:214–226, 2019.
DOI: https://doi.org/10.1177/1350650118764167.

[6] M. Takashima and N. Ohtake. "Influence of interlayer on wear and corrosion resistance of DLC film.". *Journal of Solid Mechanics and Materials Engineering*, **5**:938–944, 2011.
DOI: https://doi.org/10.1299/jmmp.5.938.

[7] T. Horiuchi, K. Yoshida, M. Kano, M. Kumagai, and T. Suzuki. "Evaluation of DLC coating damage in the delamination and wear test.". *Tribology Online*, **5**:129–135, 2010.
DOI: https://doi.org/10.2474/trol.5.129.

[8] B. D. Beake, J. S. Ling, and G. J. Leggett. "Correlation of friction, adhesion, wettability and surface chemistry after argon plasma treatment of poly (ethylene terephthalate).". *Journal of Materials Chemistry*, **8**:2845–2854, 1998.
DOI: https://doi.org/10.1039/A807261B.

[9] D. Chan and G. Stachowiak. "Review of automotive brake friction materials. ". *Proceedings of the Institution of Mechanical Engineers, Part D: Journal of Automobile Engineering*, **218**:953–966, 2004.
DOI: https://doi.org/10.1243/0954407041856773.

[10] S. Jadhav and S. Sawant. "A review paper: Development of novel friction material for vehicle brake pad application to minimize environmental and health issues.". *Materials Today: Proceedings*, **19**: 209–212, 2019.
DOI: https://doi.org/10.1016/j.matpr.2019.06.703.

[11] V. Mahale and J. Bijwe. "Exploration of plasma treated stainless steel swarf to reduce the wear of copper-free brake-pads. ". *Tribology International*, **144**:106111, 2020.
DOI: https://doi.org/10.1016/j.triboint.2019.106111.

[12] C. Chiuderi and M. Velli. "Basics of plasma astrophysics.". Springer, 2015.
DOI: https://doi.org/10.1007/978-88-470-5280-2.

[13] N. Kalel, B. Bhatt, A. Darpe, and J. Bijwe. "Argon low-pressure plasma treatment to stainless steel particles to augment the wear resistance of Cu-free brake-pads. ". *Tribology International*, **167**: 107366, 2022.
DOI: https://doi.org/10.1016/j.triboint.2021.107366.

[14] M. A. Samad, N. Satyanarayana, and S. K. Sinha. "Effect of air–plasma Pre-treatment of si substrate on adhesion strength and tribological properties of a UHMWPE film.". *Journal of Adhesion Science and Technology*, **24**:2557–2570, 2010.
DOI: https://doi.org/10.1163/016942410X508181.

[15] M. A. Samad, N. Satyanarayana, and S. K. Sinha. "Tribology of UHMWPE film on air-plasma treated tool steel and the effect of PFPE overcoat.". *Surface and Coatings Technology*, **204**:1330–8, 2010.
DOI: https://doi.org/10.1016/j.surfcoat.2009.09.011.

[16] E. M. Liston. "Plasma treatment for improved bonding: A review.".

[17] C. Hamatschek, K. Augsburg, D. Schobel, S. Gramstat, A. Stich, F. Gulden, and D. Hesse. "Comparative study on the friction behaviour and the particle formation process between a laser cladded brake disc and a conventional grey cast iron disc.". *Metals*, **13**:300, 2023.
DOI: https://doi.org/10.3390/met13020300.

[18] F. Ilie and A.-C. Cristescu. "Tribological behavior of friction materials of a disk-brake pad braking system affected by structural changes-A review.". *Materials*, **15**:4745, 2022.
DOI: https://doi.org/10.3390/ma15144745.

[19] N. Aranganathan, V. Mahale, and J. Bijwe. "Effects of aramid fiber concentration on the friction and wear characteristics of non-asbestos organic friction composites using standardized braking tests.". *Wear*, **354**:69–77, 2016.
DOI: https://doi.org/1016/j.wear.2016.03.002.

[20] M. Muthu Samy and D. Lenin Singaravelu. "Green friction: Exploring the evolution and potential of natural fibers and other brake pad ingredients in sustainable automotive engineering-A review". *Polymer Composites*, , 2024.
DOI: https://doi.org/10.1002/pc.29387.

[21] G. Sathyamoorthy, R. Vijay, and D. Lenin Singaravelu. "Brake friction composite materials: a review on classifications and influences of friction materials in braking performance with characterizations. ". *Proceedings of the Institution of Mechanical Engineers, Part J: Journal of Engineering Tribology*, **236**:1674–706, 2022.
DOI: https://doi.org/10.1177/13506501211064082.

[22] H. Rochardjo, P. Nawangsari, and A. Waskito. "Friction modifiers optimization on tribological properties of Non-asbestos organic (NAO) brake pad by DoE-Taguchi method. ". *Tribology in Industry*, **43**:310, 2021.
DOI: https://doi.org/10.24874/ti.1044.01.21.04.

[23] G. Xiao and Z. Zhu. "Friction materials development by using DOE/RSM and artificial neural network. ". *Tribology International*, **43**:218–27, 2010.
DOI: https://doi.org/10.1016/j.triboint.2009.05.019.

[24] A. I. Khuri and S. Mukhopadhyay. "Response surface methodology.". *Wiley interdisciplinary reviews: Computational statistics*, **2**:128–149, 2010.
DOI: https://doi.org/10.1002/wics.73.

[25] R. Cai, J. Zhang, X. Nie, J. Tjong, and D. Matthews. "Wear mechanism evolution on brake discs for reduced wear and particulate emissions. ". *Wear*, **452**:203283, 2020.
DOI: https://doi.org/10.1016/j.wear.2020.203283.

[26] R. Cai, C. Zhao, and X. Nie. "Alumina-based coating with dimples as enabling sustainable technology to reduce wear and emission of the brake system.". *ACS Sustainable Chemistry & Engineering*, **8**: 893–9, 2019.
DOI: https://doi.org/10.1021/acssuschemeng.9b05302.

[27] C. Bai, Z. Gong, L. An, L. Qiang, J. Zhang, G. Yushkov, A. Nikolaev, M. Shandrikov, and B. Zhang. "Adhesion and friction performance of DLC/rubber: The influence of plasma pretreatment.". *Friction*, **9**: 627–41, 2021.
DOI: https://doi.org/10.1007/s40544-020-0436-6.

[28] M. Eriksson and S. Jacobson. "Tribological surfaces of organic brake pads.". *Tribology International*, **33**:817–27, 2000.
DOI: https://doi.org/10.1016/S0301-679X(00)00127-4.

[29] W. Österle and A. Dmitriev. "Functionality of conventional brake friction materials–perceptions from findings observed at different length scales.". *Wear*, **271**:2198–207, 2011.
DOI: https://doi.org/10.1016/j.wear.2010.11.035.